Novel 1.31µm narrow-band TE-mode filter design based on a PBG shift in a 2D Photonic Crystal Slab

F. Lallam[1], H. Abri Badaoui[*2], and M. Abri[2]

[1]*STIC Laboratory, Faculty of Technology, University of Tlemcen, Algeria*
[2] *Telecommunications Laboratory, Faculty of Technology, University of Tlemcen, Algeria*

Received April 15, 2016; accepted July 18, 2016; published September 30, 2016

Abstract—In this letter, a novel 1.31µm narrow-band TE-Mode filter design has been proposed, based on a photonic band gap shift in a 2D photonic crystal slab with triangular lattice air holes, using the 2D-FDTD method to numerically model the proposed filter device. The structure is achieved by the association of three waveguides W_1^KA coupled in a cascade arrangement within the same cell of a PC with a triangular lattice with a single removed full row. A modulated Gaussian pulse is used to provide wide-band excitation at any desired position inside the computational domain of the photonic crystal. The best filter configuration performances in terms of filtering and transmission is found for 60 inclusions with a maximum of transmission around 80% localized near 1.31µm

Potential applications of photonic crystals (PCs) are extensive and cover several areas: such as production of Extremely High Q-Factor Measurement [1], experimental GVD engineering in slow light slot photonic crystal waveguides [2], tunable add/drop filter [3], de-multiplexers [4], splitters [5]-[6], new more efficient and compact optoelectronic devices reproducing the operating principles of different components of an integrated circuit, using photons as information carriers instead of electrons. They also have applications in a medical imaging field [7], measurements in nano-crystal-based solar cells [8], as well as selective filters [9], which are a promising application of two dimensional PCs; this is the subject of the present work.

The finite difference time domain (FDTD) method is regarded as a useful electromagnetic modeling tool because of its versatility [10]. The FDTD method is capable of handling inhomogeneous materials in two or three dimension forms. Since the data storage in a computer is limited by the size of memory, it is not possible to handle an open region problem directly. To mitigate this problem, the perfectly matched layer (PML) technique is widely used in the FDTD simulations; it exhibits accuracy level that is significantly better than most other absorbing boundary conditions (ABCs) [11].

This work is based on the design of devices for guiding and selective filtering PC, operating at a wavelength of 1.31µm, which corresponds to a normalized frequency $a/\lambda = 0.366$, where a represents the lattice constant. To achieve this goal, we adopted a specific methodology with consists in cascading several waveguides W_1^KA with different radii until the filter responds to our specifications. The nomenclature W_nD^A is given in [9, 12].

The first considered structure consists of an array of air cylinders holes having a radius r, in a dielectric medium with a refractive index $n_{eff} = 3.24$. This value corresponds to the effective refractive index in an InP/GaInAsP/InP heterostructure with a three-layer system [13-14]. These air rods are finitely arranged in the x and y directions and infinitely long in the z direction. In 2D dimensions, 13 parallel layers of holes are arranged in the y direction. This structure has the following parameters: $a = 0.48$µm, the filling factor $f = 0.44$ in order to obtain the suitable and desired normalized frequency $a/\lambda = 0.366$. Numerical simulations are performed for the TE polarization. We begin by implementing the spatially dispersive FDTD method in 2D simulations with a view to studying wave propagations through a PC. The computational domain has a rectangular shape in the x-y plane. According to the stability criterion [15], the spatial discretization in the FDTD simulation is chosen to be $\Delta x = \Delta y = 0.04$µm. The discretized time step is $\Delta t = \Delta x/ (2c)^{1/2}$ where c is the velocity of light in free space. A modulated Gaussian pulse is used to provide wide-band excitation at any desired position inside the computational domain comprising the CP. Note that the simulations were achieved using an Apple i7 CPU M 620 computer, with 8 Gb RAM memory. The transmission coefficient versus wavelength for the TE polarization, derived from the 2D-FDTD simulation corresponding to W_1^KA with 30 holes along the x direction and the ratio $r/a = 0.36$, is plotted in Fig. 1.a. It can be seen that large transmission achieved the values of 60% to 80%, extending over a frequency band [1.3-1.8µm]. Other modes appear such as the mode at a normalized frequency 0.309 ($\lambda = 1.55$ µm). Figure 1.b shows the spectral transmission with $r/a = 0.385$. It can be seen that the dispersion diagram is modified due to the change of holes size. Several modes appear like the 1.31 and 1.55µm peaks. Figure 1.c corresponds to W_1^KA

[*] E-mail: elnbh@yahoo.fr

having the same number of holes and the ratio r/a = 0.48. Low transmission is observed in the frequency band between 1.36 and 1.42µm, otherwise the modes are vanishing in range [1.43-1.77µm]. Moreover, the coefficient of transmission reaches its maximum at an average value of 65% at a wavelength of 1.31µm and an evanescent mode occurs at 1.55µm. This reflects the selective transmission frequency of an electromagnetic wave.

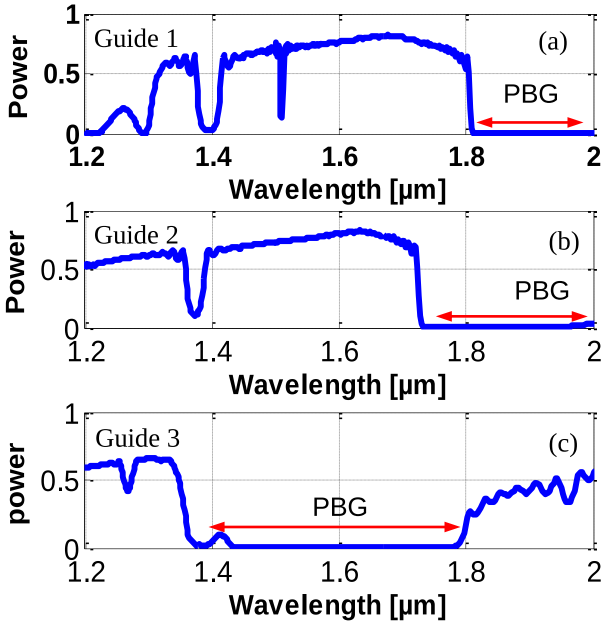

Fig. 1. Calculated transmission coefficient of W_1^KA (a) r_1/a= 0.36 (b) r_2/a= 0.385. (c) r_3/a= 0.48.

In the following, 2D-FDTD numerical simulation is done to improve the performances of the selective filter achieved by the association of three waveguides W_1^KA coupled in a cascade arrangement within the same cell of PC with a triangular lattice. The rations of each waveguide W_1^KA are respectively r_1/a = 0.36, r_2/a = 0.385 and r_3/a = 0.48 with a different number of holes N.

Table 1. Optimization parameters of different topologies.

Parameters	1st topology Fig 2. (a)	2nd topology Fig 2. (b)	3rd topology Fig 2. (c)
Total rods $n=3\times N$	30	45	60
a [µm]	0.48	0.48	0.48
r_1 [µm]	0.1728	0.1728	0.1728
r_2 [µm]	0.1848	0.1848	0.1848
r_3 [µm]	0.2304	0.2304	0.2304
w_1 [µm]	0.46	0.48	0.48
w_2 [µm]	0.36	0.36	0.36
d_1 [µm]	4.68	7.06	9.4656
d_2 [µm]	4.66	7.0896	9.4896
d_3 [µm]	4.78	7.1808	9.5808
D [µm]	4.66	4.66	4.66

The geometrical parameters after optimization shown in Fig. 2 (a) are reported in Table 1.

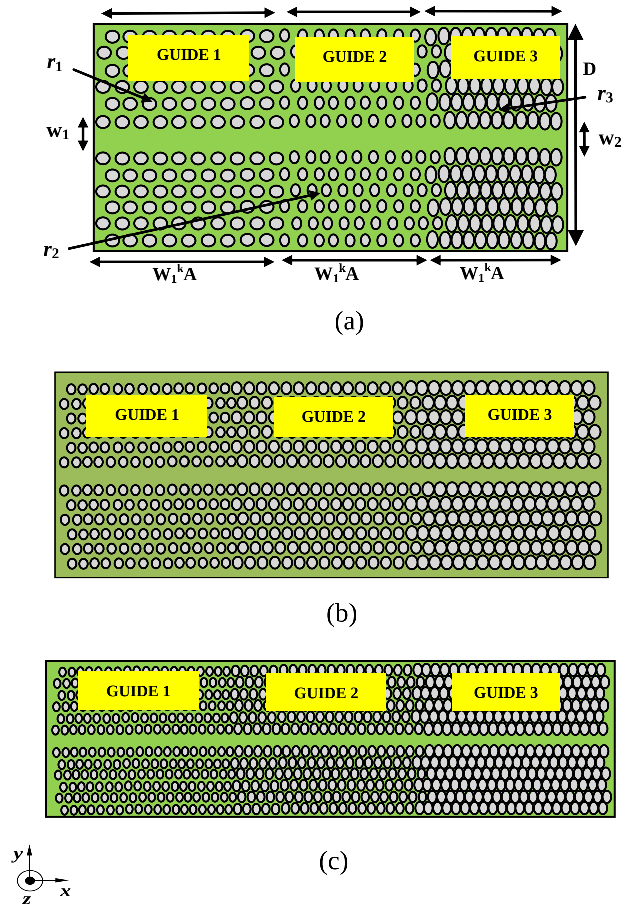

Fig. 2. Modeling scheme of a PC with association of three guides W_1^K A with a triangular lattice with r_1/a = 0.36, r_2/a = 0.385 and r_3/a = 0.48.

Figure 3 illustrates both the normalized spectra in transmission corresponding to three selective waveguides with different values of n = 30, 45 and 60 holes. All the obtained response has a suitable maximum peak localized at λ = 1.31µm with respectively 88%, 80% and 78% in the transmission peak. However, other peaks with a coefficient of transmission higher than 40% and 30% respectively occur in the frequency band [1.21-1.29] and [1.40µm-1.45µm] for the filter with n=30 rods. It is evident that single guided modes are coupled into these waveguides, though the excitation of certain modes depends highly on the symmetry of field patterns. The quality factor $Q = \Delta\lambda/\lambda_r$ (where λ_r represents the resonance wavelength and Δλ represents FWHM of the band) of each configuration is respectively 18.71, 22.78 and 29.77. Compared to two structures: N=10 for each waveguide, the total number equal to 30 (Fig. 2 a) and N = 15 for each waveguide, the total number equal to 45

(Fig. 2b), the selective filter corresponding to N = 20 for each waveguide and the total number equal to 60, (Fig. 2c) presents a significant improvement regarding the disappearance of unwanted modes around the desired frequency. We have observed that the amplitude of transmission is significantly improved by increasing the number of inclusions. So the best configuration in terms of filtering and transmission is the last topology.

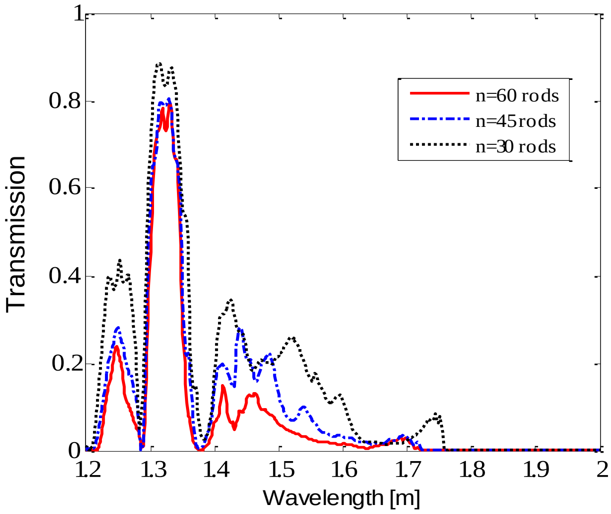

Fig. 3. Calculated transmission coefficients for the simulated selective filter for different rods.

The representation of distribution of a magnetic field inside the selective filter corresponding to the third topology with a spectral response close to the frequency 1.31µm, is reported in Fig. 4 for different step time iterations: 1500 and 11000. This figure shows the confinement of the electromagnetic field and the existence of a light-guiding phenomenon along the waveguide. On one side we can see that there is a portion of the magnetic field with an allowed frequency, belonging to the bandgap and reaching the edge of the structure. Another portion of the magnetic field has a prohibited frequency which is reflected at the level of both waveguides W_1^KA.

In conclusion, electromagnetic bandgap nanostructures and specifically PCs are presently one of the most rapidly advancing sectors in the electromagnetic domain. In this work, we carried out a study of 2D crystal photonic structures with circular air holes operating as a selective filter, composed of about three waveguides holes with different radii. We found the best performance is produced when r_1 = 0.1728µm, r_2 = 0.1848µm and r_3= 0.2304µm and the total number of inclusions is 60 in the x-direction. The maximum of transmission is around 80% localized at 1.31µm.

In further perspective, we want to consider the possibility of manufacturing the filter already simulated and achieve experimental verification. This filter can be used for optical telecommunication applications.

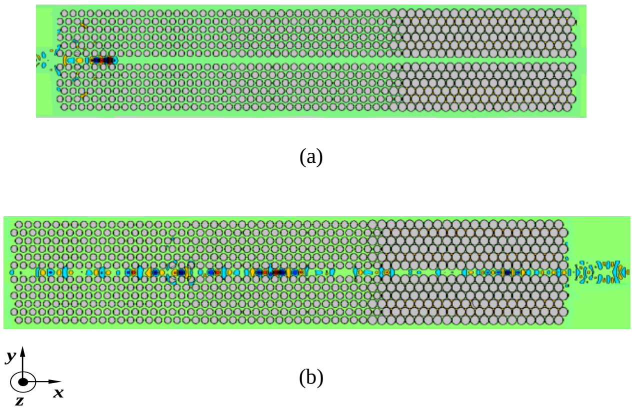

(a)

(b)

Fig. 4. Simulated distribution of a magnetic field. (a) 1500, (b) 11000 step time iteractions.

References

[1] M. Zhang, N. Liaser, IEEE Trans. Instrument. Measur. **6**, 10 (2015).
[2] S. Serna, P. Colman, W. Zhang, X. Le Roux, C. Caer, L. Vivien, E. Cassan, Scient. Reports **6**, 26956 (2016).
[3] M.A. Mansouri-Birjandi, A. Tavousi, M. Ghadrdan, Photonics Nanostr. – Fund. Appl. **21**, 44 (2016).
[4] Y. Zhuang, K. Ji, W. H. Chen, IEEE Phot. Tech. Lett **28**, 15 (2016).
[5] H. Abri Badaoui, M. Abri, Opt. Eng. **54**(6), 067104 (2015).
[6] A. Fedaouche, H. Abri Badaoui, M. Abri, IEEE Phot. Tech. Lett, **28**, 13 (2016).
[7] A. Knapitsch, E. Auffray, C.W. Fabjan, J. L. Leclercq, IEEE Trans. Nuclear Science **59**(5), 2334 (2012).
[8] M.M. Li. Weyde, D. Bozyigit, O. Yarema, V. Wood, J. Phys. Chem. C **120** (23), 12900 (2016).
[9] H. Abri Badaoui, M. Abri, Frequenz **68** (11–12), 511 (2014).
[10] C. Guiffaut, A. Reineix, International Conference on Electromagnetics in Advanced Applications (ICEAA 2015).
[11] Y. Hao, R. Mittra, *FDTD Modeling of Metamaterials: Theory and Applications* (Boston, Artech House, 2009).
[12] E. Viasnoff-Schwoob, *Propagation et Emission dans des guides multimodes a cristaux photoniques bidimensionnels* (Université Paris Sud - Paris XI, 2004).
[13] M. Svaluto Moreolo, V. Morra, G Cincotti, J. Optics A: Pure and Applied Optics, **10**, 064002 (2008).
[14] R. Ferrini, D. Leuenberger, M. Mulot, M. Qiu, J. Moosburger, M. Kamp, A. Forchel, S. Anand, R. Houdre, IEEE J. Quant. Electr. **38**, 770 (2002).
[15] A. Taflove, *Advances in Computational Electromagnetics: The Finite-Difference Time-Domain Method* (Norwood, MA: Artech House, 1998).

